

A Controllable Solid-State Ru(bpy)₃²⁺ Electrochemiluminescence Film Based on Conformation Change of Ferrocene-Labeled DNA Molecular Beacon

Xiaoying Wang, Wen Yun, Ping Dong, Jingming Zhou, Pingang He,* and Yuzhi Fang*

Department of Chemistry, East China Normal University, Shanghai 200062, P. R. China

Received August 1, 2007. In Final Form: November 20, 2007

A controllable solid-state electrochemiluminescence (ECL) film based on efficient and stable quenching of ECL of ruthenium(II) tris-(bipyridine) (Ru(bpy)₃²⁺) by oxidizing ferrocene (Fc) at the electrode is developed. The ECL intensity is correlated to the distance which is controlled by the conformation of the ferrocene-labeled DNA molecular beacon (Fc-MB) between the Fc and Ru(bpy)₃²⁺ immobilized on the electrode. The conformation adjustment is conducted *via* complementary DNA hybridizing with the bases in the loop of the Fc-MB and changing the temperature of the Fc-MB and the resultant double-stranded DNA (dsDNA). Those events all result in change of the ECL intensity. With such characteristics, the solid-state Ru(bpy)₃²⁺-ECL film has the potential to be applied to reagentless DNA ECL biosensors and to calculate thermodynamic parameters of equilibrium constants of MB binding and the stem-loop formation.

Introduction

Electrochemiluminescence (ECL), the generation of an optical signal triggered by an electrochemical reaction,¹ has attracted much attention during the past several decades due to its versatility, simplified optical setup, very low background signal, and good temporal and spatial control, and it has become an important and valuable detection method in biosensors.² Ruthenium(II) tris-(bipyridine) (Ru(bpy)₃²⁺) with the advantages of chemical stability, reversible electrochemical behavior, high luminescence efficiency, and high sensitivity under moderate conditions³ has been widely utilized in a number of bioanalytical arenas, such as immunoassays, DNA analyses, chemical sensing, imaging, and PCR product detection.^{4–10} Compared with the solution-phase Ru(bpy)₃²⁺ ECL system,^{11,12} solid-state Ru(bpy)₃²⁺-ECL film can provide several advantages, such as enhancing the ECL signal, simplifying experimental design, and creating a regenerable sensor based on Ru(bpy)₃²⁺ recycled at the electrode surface during the ECL reaction.¹³ Considerable attention has been paid to immobilize Ru(bpy)₃²⁺ on an electrode surface based on Langmuir–Blodgett technique,^{14,15} self-assembly technique,^{16,17}

and layer-by-layer (LBL) technique.¹³ Nanomaterials are utilized to fabricate ECL film recently.^{18–20} The techniques are focused on fabricating stable solid-state Ru(bpy)₃²⁺-ECL film with new immobilized materials,^{21–27} while how to combine solid-state Ru(bpy)₃²⁺-ECL film with biomolecules to make a biosensor has come to significant attention.

This paper describes fabrication of a controllable solid-state Ru(bpy)₃²⁺-ECL film by immobilization of a Ru(bpy)₃²⁺-Au nanoparticle composite on a cysteamine-derivatized Au electrode (Ru(bpy)₃²⁺-AuNPs electrode), self-assembled ferrocene-labeled DNA molecular beacon (Fc-MB), the mercaptohexyl-capped part is immobilized on the Ru(bpy)₃²⁺-AuNPs electrode while the ferrocene-labeled part can move flexibly under suitable conditions on the resultant electrode *via* Au–S interaction (Fc-MB-Ru(bpy)₃²⁺-AuNPs electrode). The ECL intensity of the film can be controlled by the conformation change of the stem-loop structure of the Fc-MB. The solid-state ECL film of Ru(bpy)₃²⁺-AuNPs composite, developed by Wang's group first,²⁸ is quite stable and has excellent ECL behavior and wonderful bioconjunction. Landers and co-workers have reported that the ferrocene molecule can quench the ECL of the Ru(bpy)₃²⁺ molecule effectively in aqueous solution.²⁹ An intramolecular ECL quenching in hybridized oligonucleotide strands has been realized to detect sequence-specific DNA using the ferrocene molecule as a quenching label on a complementary DNA sequence. On the Fc-MB-Ru(bpy)₃²⁺-AuNPs electrode, a more efficient and

* Corresponding author. Tel.: +86 21 62233508; Fax: +86 21 62233508, E-mail addresses: pghe@chem.ecnu.edu.cn (P.G. He), yzfang@chem.ecnu.edu.cn (Y.Z. Fang).

- (1) Faulkner, L. R.; Bard, A. J. *Electroanal. Chem.* **1977**, *10*, 1–95.
- (2) Fähnrich, K. A.; Pravda, M.; Guilbault, G. G. *Talanta* **2001**, *54*, 531–559.
- (3) Honda, K.; Yoshimura, M.; Rao, T. N.; Fujishima, A. *J. Phys. Chem. B* **2003**, *107*, 1653–1663.
- (4) Yu, H.; Bruno, J. G.; Cheng, T.; Calomiris, J. J.; Goode, M. T.; Gatto-Menking, D. L. *J. Biolumin. Chemilum.* **1995**, *10*, 239–245.
- (5) Honda, K.; Noda, T.; Yoshimura, M.; Nakagawa, K.; Fujishima, A. *J. Phys. Chem. B* **2004**, *108*, 16117–16127.
- (6) Chovin, A.; Garrigue, P.; Vinatier, P.; Sojic, N. *Anal. Chem.* **2004**, *76*, 357–364.
- (7) Miao, W. J.; Bard, A. J. *Anal. Chem.* **2004**, *76*, 5379–5386.
- (8) Richter, M. M. *Chem. Rev.* **2004**, *104*, 3003–3036.
- (9) Chang, Z.; Zhou, J. M.; Zhao, K.; Zhu, N. N.; He, P. G.; Fang, Y. Z. *Electrochim. Acta* **2006**, *52*, 575–580.
- (10) Zhan, W.; Bard, A. J. *Anal. Chem.* **2007**, *79*, 459–463.
- (11) White, H. S.; Bard, A. J. *J. Am. Chem. Soc.* **1982**, *104*, 6891–6895.
- (12) Jirka, G. P.; Nieman, T. A. *Microchim. Acta* **1994**, *113*, 339–347.
- (13) Guo, Z. H.; Shen, Y.; Wang, M. K.; Zhao, F.; Dong, S. J. *Anal. Chem.* **2004**, *76*, 184–191.
- (14) Lyons, C. H.; Abbas, E. D.; Lee, J. K.; Rubner, M. F. *J. Am. Chem. Soc.* **1998**, *120*, 12100–12107.
- (15) Zhang, X.; Bard, A. J. *J. Am. Chem. Soc.* **1989**, *111*, 8098–8105.
- (16) Zhang, Z.; Bard, A. J. *J. Phys. Chem.* **1988**, *92*, 5566–5569.

(17) Sun, X. P.; Du, Y.; Zhang, L. X.; Dong, S. J.; Wang, E. K. *Anal. Chem.* **2007**, *79*, 2588–2592.

(18) Zhang, L. H.; Dong, S. J. *Electrochem. Commun.* **2006**, *8*, 1687–1691.

(19) Choi, H. N.; Lee, J. Y.; Lyu, Y. K.; Lee, W. Y. *Anal. Chim. Acta* **2006**, *565*, 48–55.

(20) Lin, Z. Y.; Chen, G. N. *Talanta* **2006**, *70*, 111–115.

(21) Rubinstein, I.; Bard, A. J. *J. Am. Chem. Soc.* **1981**, *103*, 5007–5013.

(22) Khramov, A. N.; Collinson, M. M. *Anal. Chem.* **2000**, *72*, 2943–2948.

(23) Wang, H. Y.; Xu, G. B.; Dong, S. J. *Electroanalysis* **2002**, *14*, 853–857.

(24) Choi, H. N.; Cho, S. H.; Lee, W. Y. *Anal. Chem.* **2003**, *75*, 4250–4256.

(25) Ding, S. N.; Xu, J. J.; Chen, H. Y. *Electrophoresis* **2005**, *26*, 1737–1744.

(26) Sun, X. P.; Du, Y.; Zhang, L. X.; Dong, S. J.; Wang, E. K. *Anal. Chem.* **2006**, *78*, 6674–6677.

(27) Guo, S. J.; Wang, E. K. *Electrochem. Commun.* **2007**, *9*, 1252–1257.

(28) Sun, X. P.; Du, Y.; Dong, S. J.; Wang, E. K. *Anal. Chem.* **2005**, *77*, 8166–8169.

(29) Cao, W. D.; Ferrance, J. P.; Demas, J.; Landers, J. P. *J. Am. Chem. Soc.* **2006**, *128*, 7572–7578.

Table 1. Oligonucleotide Sequences Used in the Experiment

description	sequence
DNA molecular beacon ^a	5'-NH ₂ -(CH ₂) ₆ -CCCGTTGGTGTGGTTGGATTGATCGTAGGTACAACC-(CH ₂) ₆ -SH-3'
complementary sequence	3'-CACACCAACCTAACTAGCATCCAT-5'
one-base mismatched sequence	3'-CACACCAACCTAACTAGCATACAT-5'
three-base mismatched sequence	3'-CACTCCAACCTGACTAGCATACAT-5'
noncomplementary sequence	3'-AGATAAGCATACGACTGAGATTCA-5'

^a NH₂-MB-SH has a stem of five base pairs (underlined), which is stable in self-hybridized stem-loop structure under standard condition and can easily be separated when the bases in the loop hybridize with the complementary sequence.

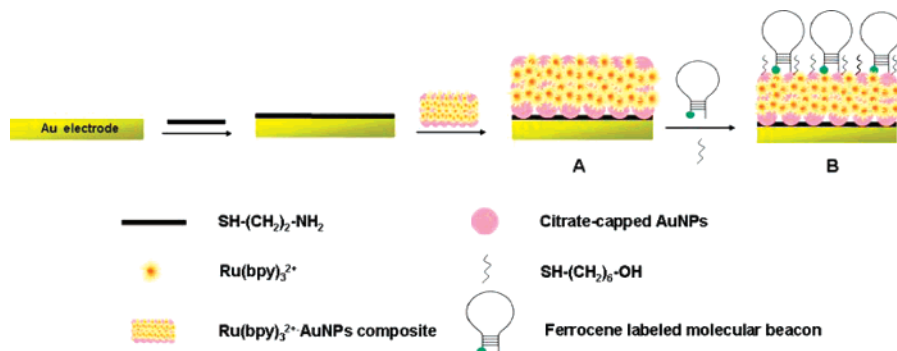


Figure 1. Schematic representation of the preparation of the Fc-MB-Ru(bpy)₃²⁺-AuNPs electrode. (A) Luminescent substrate of Ru(bpy)₃²⁺-AuNPs on Au electrode. (B) Quenching monolayer of Fc-MB-Ru(bpy)₃²⁺-AuNPs on Au electrode.

stable ferrocene quenching of ECL of Ru(bpy)₃²⁺ is obtained, because the Fc-MB is closely attached onto the Ru(bpy)₃²⁺-AuNPs composite *via* the Au-S interaction. The quenching efficiency of ECL is dependent on the distance between the ferrocene and Ru(bpy)₃²⁺ immobilized on the film. As the distance can be controlled by the conformation of the Fc-MB, the ECL intensity of the solid-state Ru(bpy)₃²⁺-ECL film changes subsequently. We attempt to adjust the conformation of the Fc-MB flexibly by different means. The ferrocene can be apart away from the Ru(bpy)₃²⁺ when the Fc-MB is hybridized with the complementary DNA to form double-stranded DNA (dsDNA) for the rigid structure of the dsDNA, or when the conformation of the Fc-MB and the resultant dsDNA are altered by temperature change. The fact of changing the quenching interaction of ferrocene on Ru(bpy)₃²⁺ finally results in controlling the ECL intensity of the film. Therefore, the controllable solid-state Ru(bpy)₃²⁺-ECL film is better than the other ECL quenching methods and can be utilized as reagentless DNA ECL biosensors.

Experimental Section

Reagents and Apparatus. Oligonucleotides were purchased from Shenggong Bioengineering Ltd Company (Shanghai, China). The oligonucleotide sequences are shown in Table 1. Ru(bpy)₃²⁺ (99.95%), HAuCl₄, 6-mercapto-1-hexanol (SH-(CH₂)₆-OH, >97.0%), cysteamine (SH-(CH₂)₂-NH₂), and 1-ethyl-3-[(3-dimethylamino)propyl]carbodiimide (EDC) were purchased from Sigma (USA). Ferrocenecarboxylic acid (FCA) was purchased from Maoji Bioengineering Ltd Company (Shanghai, China). The following buffer solutions were used: 10 mM phosphate buffer solution (PBS) containing 100 mM LiClO₄ (pH 7.3), 10 mM PBS containing 0.8 M NaCl and 100 mM LiClO₄ (pH 7.3); 20 mM PBS containing 1.0 mM tri-*n*-propylamine (TPRA) and 5.0 mM LiClO₄ (pH 8.7) was used as a detecting buffer solution. Other reagents were of analytical reagent grade. All of the solutions were prepared with ultrapure water from a Millipore Milli-Q system.

ECL was measured with MPI-E electrogenerated chemiluminescence analyzer (Xi'an Remax Electronic Science Tech. Co. Ltd); cyclic voltammetry (CV) was recorded with CHI 660A electrochemical analyzer (CHI Instruments Inc., USA).

Preparation of Fc-MB-Ru(bpy)₃²⁺-AuNPs Electrode. Figure 1 represents the procedure of preparation of the Fc-MB-Ru(bpy)₃²⁺-AuNPs electrode which has a controllable solid-state Ru(bpy)₃²⁺-

ECL film. The self-assembled monolayer of cysteamine on the Au electrode is prepared first; then, the Ru(bpy)₃²⁺-AuNPs composite is assembled onto the surface of the cysteamine-derivatized Au electrode to immobilize the luminescent substrate on the electrode surface (Figure 1A). To obtain a quenching monolayer of Fc-MB-Ru(bpy)₃²⁺-AuNPs on a Au electrode (Figure 1B), the Fc-MB is attached onto the Ru(bpy)₃²⁺-AuNPs electrode *via* Au-S interactions, and SH-(CH₂)₆-OH is dropped onto the Ru(bpy)₃²⁺-AuNPs electrode to hold the unassembled surface by the Fc-MB and to adjust the distributing degree of the Fc-MB on the electrode. The following is the detailed preparation processes.

Preparation of AuNPs and Ru(bpy)₃²⁺-AuNPs Composite. AuNPs with a diameter of 16 nm were prepared by citrate reduction of HAuCl₄ in aqueous solution according to the literature.³⁰ In brief, 100 mL of solution containing 0.01 g of HAuCl₄ was brought to reflux, and then 2.5 mL of 1% sodium citrate solution was introduced with stirring. The solution was kept boiling for 30 min and cooled to room temperature. The product was stored in a dark glass bottle at 4 °C for further use.

In a typical experiment, 150 μL of 40 mM Ru(bpy)₃²⁺ aqueous solution was added into 20 mL of the AuNPs solution under vigorous stirring at room temperature. Several minutes later, a large amount of black precipitate was formed. The resulting Ru(bpy)₃²⁺-AuNPs composite was collected by centrifugation, washed several times with water, and then suspended in water.

Synthesis of Ferrocene-Labeled DNA Molecular Beacon. Fc-MB was prepared by chemically bonding FCA to the terminal 5'-amino of the NH₂-MB-SH in the presence of a water-soluble EDC.³¹ Briefly, 20 mg of imidazole was first added into 200 μL of 1 mM FCA, and the solution was adjusted to pH 7 by 1 M HCl. EDC was then added into this prepared solution to activate those carboxylic groups on FCA. After 30 min, 280 μL of 10 μM NH₂-MB-SH was added into the resulting FCA-EDC solution with stirring. After 12 h, the reaction was stopped by adding 100 μL of 3 M sodium acetate and 1 mL of ethanol. The above solution was refrigerated for 8 h and filtered, and the sediment was obtained as Fc-MB. The final product was washed with 70% cold ethanol, centrifuged, resuspended in 10 mM PBS containing 100 mM LiClO₄ (pH 7.3), and stored at 4 °C for later use.

Formation of Luminescent Substrate of Ru(bpy)₃²⁺-AuNPs on Au Electrode. The surface of the Au electrode was polished with an

(30) Doron, A.; Katz, E.; Willner, I. *Langmuir* **1995**, *11*, 1313–1317.

(31) Yang, M. L.; Gao, L. J.; He, P. G.; Fang, Y. Z. *Chin. J. Anal. Chem.* **2005**, *10*, 1469–1472.

alumina slurry and rinsed with water and ethanol in an ultrasonic bath briefly. The Au electrode was further treated electrochemically in 0.5 M H₂SO₄ by scanning the potential from -0.2 to 1.7 V at a scan rate of 10 V s⁻¹ for 15 min until an ideal voltammogram was observed. It was soaked in 0.1 M cysteamine aqueous solution for 2 h at room temperature to form the cysteamine monolayer (cysteamine-derivatized Au electrode). After that, the electrode was thoroughly rinsed with water to remove the physically adsorbed cysteamine. A 2 μ L aliquot of the suspension of Ru(bpy)₃²⁺-AuNPs composite was placed on the cysteamine-derivatized Au electrode surface. The as-prepared electrode was air-dried at room temperature. After rinsing with water thoroughly, the luminescent substrate of Ru(bpy)₃²⁺-AuNPs was immobilized on the Au electrode surface.

Formation of Quenching Monolayer of Fc-MB-Ru(bpy)₃²⁺-AuNPs on Au Electrode. A 2 μ L aliquot of 10 μ M Fc-MB was pipetted onto the surface of Ru(bpy)₃²⁺-AuNPs immobilized Au electrode as uniformly as possible and self-assembled for 12 h at room temperature, and then the electrode was washed with 10 mM PBS containing 100 mM LiClO₄ (pH 7.3). The electrode was treated with 1.0 mM SH-(CH₂)₆-OH solution containing 100 mM LiClO₄ for 2 h to hold the unassembled surface by the Fc-MB. After rinsing thoroughly, a quenching monolayer of Fc-MB-Ru(bpy)₃²⁺-AuNPs was formed on the Au electrode surface. This Fc-MB-Ru(bpy)₃²⁺-AuNPs electrode has a controllable solid-state Ru(bpy)₃²⁺-ECL film. The electrode was sealed to avoid evaporation during the whole assembling procedure.

Controlling the ECL Intensity Change of Fc-MB-Ru(bpy)₃²⁺-AuNPs Electrode. The Fc-MB-Ru(bpy)₃²⁺-AuNPs electrode was incubated in 500 μ L of 10 mM PBS (pH 7.3) containing 0.8 M NaCl, 100 mM LiClO₄, and different concentrations of oligonucleotide at room temperature for 2 h. Then, the electrode was washed thoroughly with the same buffer to remove the unhybridized DNA. The dsDNA electrode was formed.

The Fc-MB-Ru(bpy)₃²⁺-AuNPs electrode and the above dsDNA electrode were melted for 30 min in 10 mM PBS containing 100 mM LiClO₄ (pH 7.3), varying the temperature from 10 $^{\circ}$ C to 100 $^{\circ}$ C, respectively. ECL signals were measured at intervals of 10 $^{\circ}$ C.

Electrogenerated Chemiluminescence Detection. The ECL was performed in a 10 mL homemade quartz cell. A three-electrode system was used at room temperature with modified Au electrode (2 mm in diameter) as the working electrode, an Ag/AgCl (sat.) as the reference electrode, and a platinum wire as the counter electrode. Cyclic voltammetry mode with continuous potential scanning from 0.0 to 1.2 V and scanning rate of 0.1 V s⁻¹ was applied to achieve ECL signal in 20 mM PBS containing 1.0 mM TPrA and 5.0 mM LiClO₄ (pH 8.7). A high voltage of -800 V was supplied to the photomultiplier to determine the luminescence intensity. The ECL and CV curves were measured simultaneously.

Results and Discussion

Characterization of Controllable Solid-State Ru(bpy)₃²⁺-ECL Film. The corresponding ECL intensity-potential curves of the various electrodes in 20 mM PBS containing 1.0 mM TPrA and 5.0 mM LiClO₄ are presented in Figure 2. No ECL signal is obtained on a bare Au electrode (Figure 2a). A strong ECL signal appears when the luminescent substrate of Ru(bpy)₃²⁺-AuNPs was immobilized on a Au electrode (Figure 2b), while a sharp decrease of the ECL signal is observed when the quenching monolayer of ferrocene was formed on the Ru(bpy)₃²⁺-AuNPs electrode (Figure 2c). The results verify that the ECL of the Ru(bpy)₃²⁺-AuNPs can be efficiently quenched by the Fc-MB. The mechanism for quenching ECL has been explained as bimolecular energy or electron transfer between Ru(bpy)₃²⁺ and ferrocium (Fc⁺), the oxidized species of Fc, along with suppression of radical reactions.²⁹

Obviously, the quenching efficiency of the ECL of Ru(bpy)₃²⁺ is dependent on the coverage of the Fc-MB on the electrode surface. According to the method suggested by Steel et al.,³²⁻³⁴ the coverage of the DNA on electrode surface can be calculated

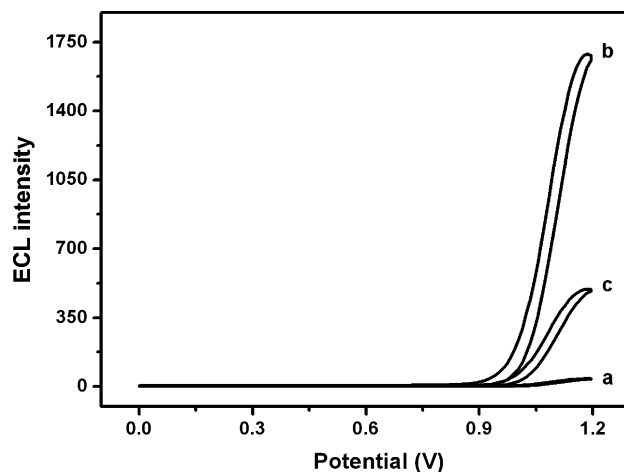


Figure 2. ECL intensity-potential curves for various electrodes in 20 mM PBS containing 1.0 mM TPrA and 5.0 mM LiClO₄ (pH 8.7). Scan rate: 0.1 V s⁻¹. Scan range: 0.0-1.2 V. (a) Bare Au electrode, (b) Ru(bpy)₃²⁺-AuNPs electrode, (c) Fc-MB-Ru(bpy)₃²⁺-AuNPs electrode.

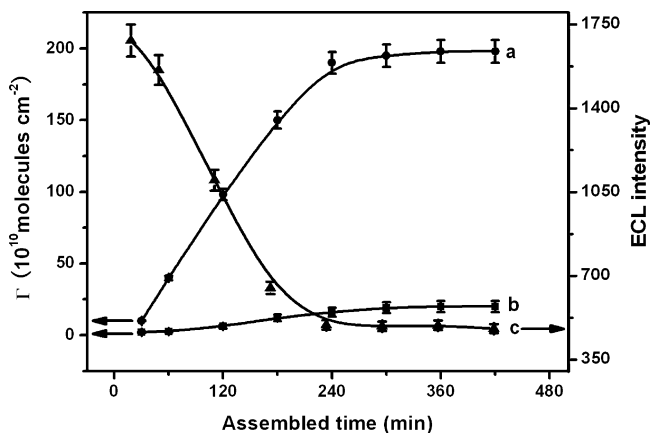


Figure 3. The average of surface coverage of the Fc-MB on (a) Ru(bpy)₃²⁺-AuNPs electrode, (b) bare Au electrode with self-assembled time, (c) ECL signals of the Fc-MB-Ru(bpy)₃²⁺-AuNPs electrode with self-assembled time.

by measuring the number of cationic redox molecules, such as tris(2,2'-bipyridyl)cobalt(III) perchlorate, electrostatically associated with the anionic DNA backbone. The method is used to estimate the average of surface coverage of the Fc-MB on the Ru(bpy)₃²⁺-AuNPs electrode and the bare gold electrode, respectively. Figure 3 shows the average of surface coverage of the Fc-MB with self-assembly time for the Ru(bpy)₃²⁺-AuNPs electrode and the bare gold electrode. The results indicate that the average of surface coverage of the Fc-MB increases steeply during the first 3 h and then gently on the Ru(bpy)₃²⁺-AuNPs electrode (Figure 3a). Compared with the average of surface coverage of the Fc-MB on the bare gold electrode (Figure 3b), the surface coverage on the Ru(bpy)₃²⁺-AuNPs electrode is approximately 10 times larger than that on the bare gold electrode. It benefits from the much higher surface area of AuNPs on the Ru(bpy)₃²⁺-AuNPs electrode. As shown in Figure 3c, the ECL signals of the Fc-MB-Ru(bpy)₃²⁺-AuNPs electrode are synchronously decreased with the increment of surface coverage of the Fc-MB. It means that the quenching efficiency of ECL of

(32) Steel, A. B.; Herne, T. M.; Tarlov, M. J. *Anal. Chem.* **1998**, *70*, 4670-4677.

(33) Cai, H.; Xu, C.; He, P. G.; Fang, Y. Z. *J. Electroanal. Chem.* **2001**, *510*, 78-85.

(34) Bard, A. J.; Faulkner, L. R. *Electrochem. Methods* **1980**, 199-206.

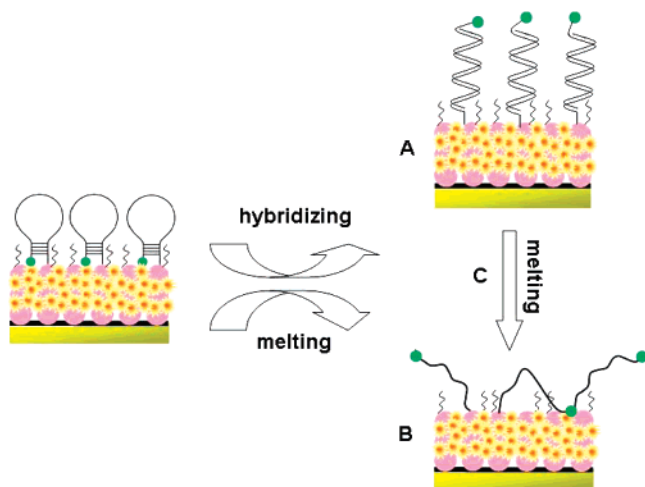


Figure 4. Schematic representation of the change of ECL intensity of the Fc-MB-Ru(bpy)₃²⁺-AuNPs electrode with the conformation change of the Fc-MB. Inducement of conformation changes of the Fc-MB by hybridization (A), the Fc-MB by temperature (B), and the resultant dsDNA by temperature (C).

Ru(bpy)₃²⁺ is dependent on the surface coverage of the Fc-MB on the electrode surface. Greater than 70% quenching efficiency of ECL of Ru(bpy)₃²⁺ has been obtained when the Ru(bpy)₃²⁺-AuNPs electrode was assembled in the 10 μM Fc-MB for about 5 h.

Change of ECL Intensity of Fc-MB-Ru(bpy)₃²⁺-AuNPs Electrode with the Conformation Change of Fc-MB. The ferrocene molecule can efficiently quench the ECL of Ru(bpy)₃²⁺ when the Fc-MB monolayer approaches the surface of Ru(bpy)₃²⁺-AuNPs, while the quenching of the ECL of Ru(bpy)₃²⁺ will become very weak if the ferrocene molecule is apart away from the Ru(bpy)₃²⁺. The distance between the ferrocene of the Fc-MB and Ru(bpy)₃²⁺-AuNPs can be controlled by changing conformation of the stem-loop structure of the Fc-MB. Figure 4 presents an illustration of the conformation change of the stem-loop structure of the Fc-MB. The stem of the Fc-MB is separated when the bases in the loop of the Fc-MB hybridize with the complementary DNA, and the rigid dsDNA structure formed. As a result, the ferrocene molecule moves away from the surface of Ru(bpy)₃²⁺-AuNPs (Figure 4A). Similarly, the stem-loop structure of the Fc-MB can be opened and lead the ferrocene molecule to move away from the surface of Ru(bpy)₃²⁺-AuNPs with the increase of the temperature of the Fc-MB-Ru(bpy)₃²⁺-AuNPs electrode (Figure 4B), resulting in a remarkable change of ECL signal. Furthermore, when the temperature of the dsDNA electrode increases, the rigid structure of the resultant dsDNA strand can also be destabilized and gradually destroyed. The conformation of the Fc-MB changes subsequently, which finally leads to the change of ECL intensity of the solid-state Ru(bpy)₃²⁺-ECL film (Figure 4C).

Figure 5 demonstrates that the corresponding ECL intensity-potential curves of the Fc-MB-Ru(bpy)₃²⁺-AuNPs electrodes after they are incubated in complementary DNA, one-base mismatched DNA, three-base mismatched DNA, or noncomplementary DNA solution, respectively. In comparison with the ECL signal of the Fc-MB-Ru(bpy)₃²⁺-AuNPs electrode without hybridization with any DNA (Figure 5a), there is a remarkable enhancement of the ECL signal of the Fc-MB-Ru(bpy)₃²⁺-AuNPs electrode after the process of hybridization with complementary DNA (Figure 5e). The enhancement is in direct proportion with the concentration of the complementary DNA (Figure 5e,f), while the changes of the ECL signal of the Fc-MB-Ru(bpy)₃²⁺-AuNPs electrode are almost negligible after the process of hybridization

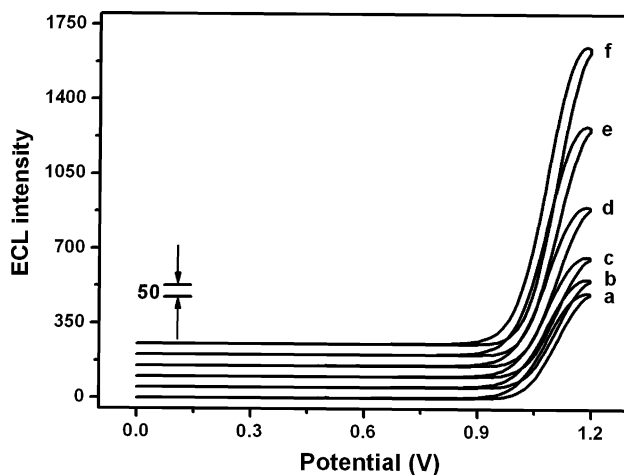


Figure 5. ECL intensity-potential curves for various electrodes in 20 mM PBS containing 1.0 mM TPrA and 5.0 mM LiClO₄ (pH 8.7). Scan rate: 0.1 V s⁻¹. Scan range: 0.0–1.2 V. (a) Fc-MB-Ru(bpy)₃²⁺-AuNPs electrode; Fc-MB-Ru(bpy)₃²⁺-AuNPs electrode hybridization with any DNA (b) 10 nM noncomplementary DNA, (c) 10 nM three-base mismatched DNA, (d) 10 nM one-base mismatched DNA, (e) 10 nM complementary DNA, and (f) 1 μM complementary DNA, respectively.

with the three-base mismatched DNA (Figure 5c) or noncomplementary DNA (Figure 5b). Meanwhile, the one-base mismatched DNA (C/A mismatched) turns out to be about 44% signal from the complementary DNA, when they are in the same concentration (Figure 5d). Therefore, the characteristics of the controllable solid-state ECL film of Fc-MB-Ru(bpy)₃²⁺-AuNPs have the potential for reagentless ECL biosensors to recognize and detect sequence-specific DNA.

As we all know, the stability of the stem-loop structures and that of the probe-target duplex *via* the free energies accompanying their formation are generally used for MBs evaluation. However, MBs can also be handily characterized, according to the melting-point temperature (*T*_m, defined as the temperature at which half of the double-helical structure of DNA is denatured) of the stem-loop structure and that of the resultant duplex.³⁵ The characteristics of ECL of Ru(bpy)₃²⁺ with temperature change of the Fc-MB-Ru(bpy)₃²⁺-AuNPs electrode were investigated by varying the temperature according to the reported procedures.³⁶ Figure 6 shows the ECL intensity-temperature curves for Fc-MB-Ru(bpy)₃²⁺-AuNPs electrode unhybridized or hybridized with various DNA. As shown in curve a of Figure 6, for the Fc-MB-Ru(bpy)₃²⁺-AuNPs electrode without hybridization with any DNA, a smaller ECL signal is maintained below 20 °C; from 30 °C, the ECL signals start to increase and the enhancement gradually becomes fast after 50 °C; then, after 70 °C the ECL signal peaks and then reduces a little. The scheme of the hypothetical temperature-induced transitions (Figure 7a) can explain the process. Below 20 °C, the Fc-MB keeps a stem-loop structure that ensures approach of the ferrocene molecule to the surface of Ru(bpy)₃²⁺-AuNPs and quenches the ECL of Ru(bpy)₃²⁺. The stem structure and internal secondary structure become destabilized and gradually open when the temperature increases, and at 70 °C, the stem structure is completely opened to a chainlike strand, resulting in the ferrocene molecule being far apart from the Ru(bpy)₃²⁺, and the quenching of the ECL of Ru(bpy)₃²⁺ becomes weak. The reason the ECL signal was reduced a little after 70 °C may be that a little of

(35) Szemes, M.; Schoen, C. D. *Anal. Biochem.* **2003**, *315*, 189–201.

(36) Jenkins, D. M.; Chami, B.; Kreuzer, M.; Presting, G.; Alvarez, A. M.; Liaw, B. Y. *Anal. Chem.* **2006**, *78*, 2314–2318.

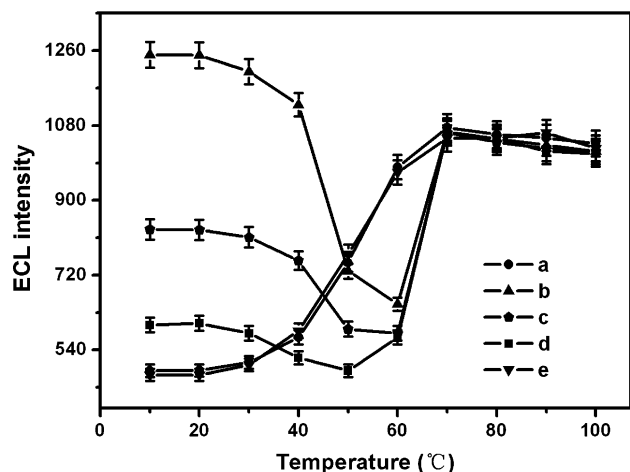


Figure 6. ECL intensity–temperature curves for (a) unhybridized Fc-MB-Ru(bpy)₃²⁺-AuNPs electrode, hybridized Fc-MB-Ru(bpy)₃²⁺-AuNPs electrodes with (b) complementary DNA, (c) one-base mismatched DNA, (d) three-base mismatched DNA, and (e) noncomplementary DNA incubated in 10 mM PBS containing 100 mM LiClO₄ (pH 7.3) for 30 min with varying temperature from 10 to 100 °C.

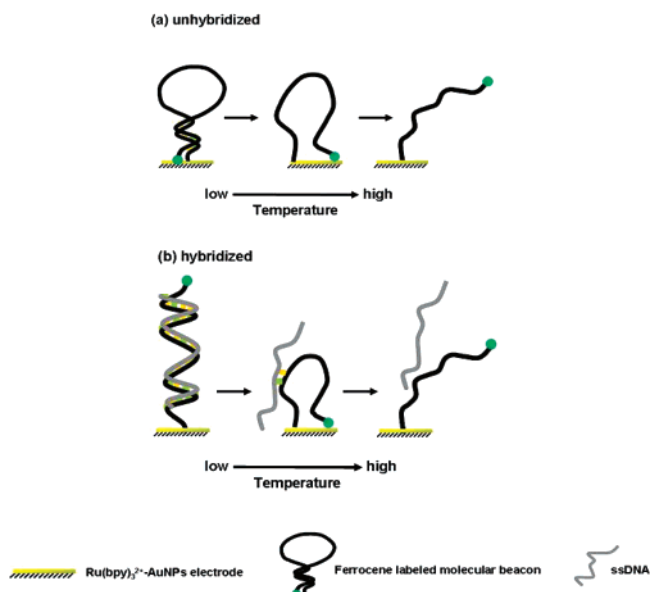


Figure 7. Hypothetical temperature-induced transitions in conformation of the Fc-MB for (a) unhybridized and (b) hybridized molecules.

Ru(bpy)₃²⁺-AuNPs are lost from the surface of the gold electrode. Therefore, the T_m of the Fc-MB is estimated at around 60 °C, which is similar to the calculated and reported results.^{37,38}

On the other hand, when the Fc-MB-Ru(bpy)₃²⁺-AuNPs electrode hybridized with the complementary DNA, the rigid dsDNA strands are formed on the surface of the Fc-MB-Ru(bpy)₃²⁺-AuNPs electrode, the strongest ECL signal of Ru(bpy)₃²⁺ is observed below 20 °C, then the ECL signals decrease below 60 °C, and finally, the ECL signals reversely increase and peak and then reduce a little with the temperature increase (Figure 6b). Similarly, The scheme of the hypothetical temperature-induced transitions in Figure 7b can explain the ECL intensity–temperature curve of the hybridized Fc-MB-Ru(bpy)₃²⁺-AuNPs

electrode. The ECL signal of the resultant dsDNA electrode at low temperature is higher than that of the Fc-MB-Ru(bpy)₃²⁺-AuNPs electrode at 70 °C, because the rigid structure of the dsDNA strand leads the ferrocene molecule of the Fc-MB to be farther away from the Ru(bpy)₃²⁺ than the chainlike Fc-MB strand. With the increase of temperature, the dsDNA structure is gradually denatured and a destabilized stem-loop structure of the Fc-MB is reformed, resulting in higher quenching of the ECL of Ru(bpy)₃²⁺; while at higher temperature (over 70 °C), the complementary DNA leaves from the loop of the Fc-MB, and the destabilized stem-loop structure of the Fc-MB is completely opened to become a chainlike strand, conducive to a reverse increase of the ECL signal. Therefore, the T_m of the corresponding dsDNA should be the point at which half of the structure of dsDNA is denatured and the destabilized stem-loop structure of the Fc-MB is reformed, namely, the lowest point of ECL signal in the ECL intensity–temperature curve. Because of the experimental precision, the T_m of the corresponding dsDNA is roughly predicted to be approximately 60 °C.

The trends of the one-base mismatched DNA and the three-base mismatched DNA are the same as that of the complementary DNA. Due to the lower hybridization efficiency of the one-base mismatched DNA and the three-base mismatched DNA, the ECL signals of the one-base mismatched DNA and the three-base mismatched DNA are lower than that of the complementary DNA at the beginning temperature (Figure 6c,d). For the one-base mismatched DNA, the ECL signals decrease below 50 °C, while the ECL signals are almost the same at 50 °C and 60 °C. So, the bottom of ECL intensity in ECL intensity–temperature curves is supposed to be between 50 and 60 °C, which is estimated at around 55 °C (Figure 6c). The difference of temperature between the complementary DNA and the one-base mismatched DNA at the bottom of ECL intensity in the ECL intensity–temperature curves (Figure 6b,c) is about 5 °C, while the difference between the complementary DNA and the three-base mismatched DNA is about 10 °C (Figure 6b,d). All of the above can be partially explained by the thermodynamic stabilities predicted for the pairings using software tools available on the Internet (RNAssoft).³⁹ So, the T_m of the corresponding dsDNA obtained from the one-base mismatched DNA is roughly predicted to be around 55 °C, while that of dsDNA obtained from the three-base mismatched DNA is around 50 °C. The target sequence could be easily distinguished from the one-base mismatched DNA, since the difference of their T_m reaches about 5 °C. The three-base mismatched DNA was observed to melt at an even lower temperature because of the low degree of homology between it and the target sequences.³⁶ These simulations predict substantial differences in melting temperatures for the different complexes, supporting the use of temperature control to discriminate nonspecific binding effects from the target. The trend of the noncomplementary DNA is the same as that of the unhybridized Fc-MB-Ru(bpy)₃²⁺-AuNPs electrode (Figure 6e). Therefore, nonspecific interfering sequences are distinguished from the actual target sequence.

Conclusions

A controllable solid-state electrochemiluminescence film through the combination of immobilization method involving AuNPs and Ru(bpy)₃²⁺ with efficient and stable quenching of ECL of Ru(bpy)₃²⁺ by Fc as well as the flexible adjustment of DNA molecular beacon's conformation is developed. The adjustment is conducted *via* the hybridization between the

(37) Breslauer, K. J.; Frank, R.; Blöcker, H.; Marky, L. A. *Proc. Natl. Acad. Sci. U.S.A.* **1986**, *83*, 3746–3750.

(38) Xu, Y.; Yang, L.; Ye, X. Y.; He, P. G.; Fang, Y. Z. *Electroanalysis* **2006**, *18*, 873–881.

(39) Andronescu, M.; Aguirre-Hernandez, R.; Condon, A.; Hoos, H. H. *Nucleic Acids Res.* **2003**, *31*, 3416–3422.

complementary DNA and the Fc-MB and the temperature change of the Fc-MB or the resultant dsDNA. Those events all result in change of the ECL intensity. Inducement of conformation change of the Fc-MB by hybridization can be used as reagentless DNA ECL biosensors to recognize or detect sequence-specific DNA. Inducement of conformation change of the Fc-MB and the resultant dsDNA by temperature can provide a certain experimental basis for the stability of the MB stem-loop structures and that of the probe–target duplex *via* the free energies accompanying their formation. In addition, the system has the potential to be applied to the selected recognition of numerous kinds of biomolecules and to calculate thermodynamic parameters

of the equilibrium constants of MB binding because of the special matching and capturing mode between the Fc-MB and a variety of biomolecules.

Acknowledgment. We thank the National Nature Science Foundation of China (Grant No. 20675031), and Shanghai Science and Technology Committee (Grant No. 051409007 and 06PJ14032) for financial support of this work.

Supporting Information Available: Additional information. This material is available free of charge via the Internet at <http://pubs.acs.org>.

LA702345P